Available online at www.sciencedirect.com
SCIENCE DIRECT®
Journal of Catalysis 219 (2003) 305–309
JOURNAL OF CATALYSIS
www.elsevier.com/locate/jcat

# Catalytic studies on ceria lanthana solid solutions III. Surface segregation and solid state studies

M.F. Wilkes, P. Hayden, and A.K. Bhattacharya *

*Warwick Process Technology Group, Department of Engineering, University of Warwick, Coventry CV4 7AL, UK*

Received 9 January 2003; accepted 27 January 2003

**Abstract**

As part of a catalytic study, the bulk structure and surface compositions of the mixed oxides of ceria and lanthana, $Ce_{1-x}La_xO_{2-x/2}$, have been studied over the entire range of compositions. Between $x = 0$ and $x = 0.6$, the system forms solid solutions with the cubic fluorite structure. Beyond $x = 0.9$, it forms solid solutions with the hexagonal close-packed structure characteristic of lanthana. No phase characterisation was possible between $x = 0.6$ and $x = 0.9$. Lanthanum is preferentially segregated at the surface from bulk compositions up to $x = 0.9$, but further increments of lanthana cause the system to exhibit preferential surface segregation of the cerium moiety. The preparative procedure is shown to establish stationary state surface compositions, enabling classification of the composition data as segregation isotherms. Over the composition ranges of the two solid solutions, that is, $x = 0$–$0.6$ and $x = 0.9$–$1$, the surface segregation may be quantitatively described by power laws similar to the Freundlich gas adsorption isotherm.


*Keywords:* Ceria; Lanthana; Solid solution; Surface; Segregation; Isotherm

## 1. Introduction

The catalytic activities of pure and doped ceria have been variously associated with, for example, interstitial oxides [1], lattice oxygen atoms [2], oxyanion vacancies [3], basicity of the surface [4], and redox activity [5]. We have studied the activity of the catalytic combustion of methane and carbon monoxide as functions of the complete range of compositions of ceria–lanthana mixed oxides [6]. None of the existing theoretical treatments of catalytic activity, based on the character of the bulk materials, proved to be satisfactory. Since catalysis is primarily a surface phenomenon with limited involvement of the bulk, we have focused on correlating catalytic activity with the composition and nature of the surface of these mixed oxides [7]. The complete family of ceria–lanthana mixed oxides was prepared by co-precipitation and calcination of bicarbonates. Powder X-ray diffraction (XRD) was applied to identify the composition ranges forming solid solutions and calcination regimes that provide adequate stabilisation of the crystallite size for the catalytic studies. This was supported with measurement, by X-ray photoelectron spectroscopy (XPS), of the stationary state surface compositions of sintered solid solutions: one range based on the ceria structure and the other on lanthana. The resulting segregation isotherms imply strong energetic variation of adsorption sites. The surface segregation data and its quantitative modelling in terms of a non-Arrenhenius isotherm derived from statistical thermodynamics has been fully reported [6]. However, such an analysis results in cumbersome equations that are not very practical for designing catalysts. Accordingly, the same experimental data has, with less precision, here been alternatively modelled in terms of an empirical Freundlich-style isotherm.

## 2. Experimental and methods

### 2.1. Materials

Cerium(III) nitrate hexahydrate ($Ce(NO_3)_3 \cdot 6H_2O$, 99.99%, Alfa) and lanthanum(III) nitrate hexahydrate ($La(NO_3)_3 \cdot 6H_2O$, 99.999%, Aldrich) were dissolved in water to form 1 M solutions, admixed in due proportions

* Corresponding author.
*E-mail address:* akb@warwick.ac.uk (A.K. Bhattacharya).

0021-9517/$ – see front matter © 2003 Published by Elsevier Inc.
doi:10.1016/S0021-9517(03)00046-0

for the required cerium lanthanum oxide, $Ce_{1-x}La_xO_{2-x/2}$, and precipitated as their bicarbonates with excess 2 M $NH_4HCO_3$ solution. Separated by vacuum filtration, the precipitates were repeatedly washed by re-dispersion in distilled water until free of alkali, vacuum-filtered, and dried for 16 h at 383 K. The dried bicarbonates were heated in air for 2 h at 723 K. The resulting oxides were calcined in air at various temperatures in the range 873–1673 K for various periods in the range 0.1–100 h.

The time dependency of surface segregation was examined at the lanthanum concentration corresponding to the bulk stoichiometry $Ce_{0.75}La_{0.25}O_{1.875}$. This lanthanum concentration was selected since it was near the middle of the solid solution range and was of particular interest in a parallel catalytic study. The calcination temperature was 1073 K. Four aliquots (1 g) of a common preparation were calcined in alumina boats for 0.1, 1, 10, and 100 h.

The temperature dependency of surface segregation was examined at a single lanthanum concentration corresponding to the bulk stoichiometry $Ce_{0.8}La_{0.2}O_{1.9}$. Aliquots (1 g) of a common preparation were calcined in alumina boats for 8 h at 873, 1073, 1273, 1473, and 1673 K. In each case the samples were introduced into the furnace at 473 K, heated to the requisite temperature over 2 h, and held at temperature for 8 h. Cooling was effected over 2 h to 473 K and thence over a few minutes to room temperature.

To investigate the effect of bulk composition, samples of the due mixed oxides were calcined in 2-g aliquots for 8 h at 1073 K, the furnace temperature being increased and decreased with time as defined above for the temperature dependency study. A systematic series of samples were prepared where the level of lanthanum in the bulk material was varied between $0 < x < 1.0$.

### 2.2. Characterisation of the bulk

An XRD analysis was conducted for all samples using a Phillips PW1830 instrument. A Cu-$K_\alpha$ source was used, with a software subtraction of $K_{\alpha_2}$. Scans were effected over a range of $2\theta$ from 10°–80° over a 1-h period and were compared with standard library patterns for phase analysis. Lattice parameters were calculated and averaged over four peaks using the cubic model; *hkl* values for given peaks were identified by comparison with reference patterns in Phillips Electronic Instruments, CD-ROM database (1987). Crystallite size estimations were effected using the Scherrer method using XRD line-broadening data.

### 2.3. Determination of surface composition

XPS analysis was carried out using two separate instruments: measurements on the effect of temperature were made on a Kratos XSAM instrument; measurements on the effect of bulk composition and calcination time were made on a VG ESCAlab Mk II/III instrument.

Lanthanum and cerium were quantified by measurement of the element characteristic peak ($Ce_{3d}$ and $La_{3d}$) areas following subtraction of a Shirley-type background. To ensure the analysis was sufficiently specific to the surface, the X-ray source was a Mg-$K_\alpha$ X-ray source rather than an Al$K_\alpha$ source. Relative sensitivities for the elements were calculated, taking into account the photoelectron cross section [8], angular asymmetry parameter [9], energy dependence of the inelastic mean free path [10], and transmission of the energy analyser [11].

## 3. Results

### 3.1. The course of solution, crystallite growth, and segregation

In calcinations at 1073 K, lattice parameters and crystallite sizes of the mixed oxides $Ce_{1-x}La_xO_{2-x/2}$ ($x = 0$ and 0.25) were monitored over calcination times from 0.1 to 100 h. XRD shows each product to have the cubic fluorite structure. The mixed oxides exhibited peak shifts toward lower $2\theta$ values compared with pure ceria, confirming that the lanthanum was incorporated into the ceria lattice. Table 1 shows the lattice parameter increased from an average value of $5.403 \pm 0.007$ Å for pure ceria to $5.488 \pm 0.007$ Å for the mixed oxide, in good agreement with literature values [12,13]. Details of the crystallite growth are included. The lattice parameter changed little after calcination at 1073 K for 1 h, whereas some 10 h were required to achieve a marked deceleration of the sintering process. In similar calcinations, the time dependencies of the surface compositions of mixed oxides where $x = 0.25$ and $x = 0.5$ are presented in Table 2. In both cases the surface was significantly enriched with lanthanum in comparison with the bulk composition, reaching essentially stationary states after about 8 h. It was concluded that the lattice parameter and surface composition were essentially constant after a calcination period of 8–10 h at 1073 K.

Table 1
Lattice parameters and crystallite size of $CeO_2$ and $Ce_{0.75}La_{0.25}O_{1.875}$ as functions of calcination time at 1073 K

| Time (h) | $x$ | Lattice parameter (Å) | Crystallite size (nm) |
|---|---|---|---|
| 0.1 | 0 | 5.402 | 19.2 |
| 1 | 0 | 5.406 | 45.9 |
| 10 | 0 | 5.405 | 58.3 |
| 100 | 0 | 5.399 | 62.5 |
| 0.1 | 0.25 | 5.487 | 9.4 |
| 1 | 0.25 | 5.489 | 16.0 |
| 8 | 0.25 | 5.487 | 17.1 |
| 10 | 0.25 | 5.486 | 18.9 |
| 50 | 0.25 | 5.489 | 20.0 |
| 100 | 0.25 | 5.492 | 21.3 |

Table 2
Surface composition as a function of calcination time at 1073 K for the mixed oxides where $x = 0.25$ and 0.5

| Calcination time (h) | Ionic fraction of surface lanthanum (bulk $x = 0.25$) | Ionic fraction of surface lanthanum (bulk $x = 0.5$) |
|---|---|---|
| 0.1 | 0.48 | 0.71 |
| 1 | 0.50 | 0.77 |
| 8 | 0.53 | 0.78 |
| 10 | 0.53 | 0.77 |
| 50 | 0.53 | 0.78 |
| 100 | 0.53 | 0.79 |

Table 3
The influence of temperature on the crystallite sizes of $CeO_2$ and $Ce_{0.8}La_{0.2}O_{1.9}$ at calcination times of 8 h

| Calcination temperature (K) | Crystallite size (Å) of ceria | Crystallite size (Å) of $Ce_{0.8}La_{0.2}O_{1.9}$ |
|---|---|---|
| 723 (Decomposition only) | 92 | 61 |
| 773 | 105 | 66 |
| 873 | 148 | 83 |
| 973 | 218 | 119 |
| 1073 | 386 | 172 |
| 1173 | 555 | 235 |
| 1273 | 827 | 303 |
| 1373 | 1012 | 378 |

### *3.2. The effect of temperature on sintering and surface composition*

#### *3.2.1. Crystallite growth*

The temperature dependence of the growth in crystallite size for the cases of $CeO_2$ and $Ce_{0.8}La_{0.2}O_{1.9}$ is shown in Table 3: the gradients of logarithms of crystallite size versus reciprocal absolute temperature of calcination may be expressed as an apparent activation of crystallisation of about 28 kJ mol$^{-1}$.

#### *3.2.2. Segregation as a function of calcination temperature*

The temperature dependency of surface composition for bulk compositions where $x = 0.2$ and 0.5 are presented in Table 4. XRD analysis showed all the calcinates to have the cubic fluorite structure. The widely adopted model of a two-component substitional solid solution comprising a segregated surface monolayer in equilibrium with a bulk of constant composition generates the relationship

$$\frac{X_s^2}{X_s^1} = \frac{X_b^2}{X_b^1} \exp^{(-\Delta H_{Seg}/RT)},$$

where $X_s^2$ and $X_s^1$ are the atomic fractions of the segregated solute and solvent, respectively, $X_b^2$ and $X_b^1$ are the atomic fractions of the solute and solvent in the bulk solid solution, respectively; and $\Delta H_{seg}$ is the enthalpy of segregation [14]. Analysis of the data in Table 4 in terms of this equation results in an apparent enthalpy of segregation of about 7 kJ mol$^{-1}$—a coefficient much lower than that reported in an earlier study [15], where the results were interpreted in terms of an activation energy of the segregation process. However, co-precipitation is difficult to control and produces inhomogeneous solids well populated with macrodefects offering scope for a variety migratory pathways, some very facile. From the effects of time and temperature it is concluded that the surface segregation process is not limited in rate by crystallite growth.

Table 4
Surface composition of $Ce_{1-x}La_xO_{2-x/2}$ for $x = 0.2$ and 0.5 following calcinations for 8 h at various temperatures

| Calcination temperature (K) | Lanthanum surface fraction ($x = 0.2$ bulk material) | Lanthanum surface fraction ($x = 0.5$ bulk material) |
|---|---|---|
| 724 (decomposition only) | – | 0.64 |
| 873 | 0.29 | 0.73 |
| 1073 | 0.33 | 0.77 |
| 1273 | 0.36 | 0.79 |
| 1473 | 0.38 | 0.80 |
| 1673 | 0.39 | 0.83 |

### *3.3. The effect of oxide composition on the bulk structures and on surface compositions*

#### *3.3.1. Bulk structure*

The lattice parameters and crystallite sizes of a whole range of mixed oxides, $Ce_{1-x}La_xO_{2-x/2}$, where $x$ was varied from 0 to 1 and calcined at 1073 K were measured by XRD. The well-known cubic fluorite structure of ceria was the sole constituent of the XRD patterns between $x = 0$ and $x = 0.6$. XRD peaks not characteristic of the cubic fluorite phase first become apparent at $x = 0.7$. It is concluded that the solid solution limit of lanthana in ceria is about 60% ($x = 0.6$) atomic fraction of lanthanum—a result in agreement with literature values [12,16]. The progressive shift of the cubic fluorite peaks toward lower $2\theta$ values as $x$ is increased from 0 to 0.6 is attributed to expansion of the ceria lattice caused by the dissolution of the larger ions of the lanthana solute. The lattice parameters are presented in Fig. 1a where the near-linearity in the range $0 < x < 0.6$ is consistent with Vergard's Law [17]. The inflection between $x = 0.5$ and $x = 0.6$ is a further indication that the solid solution limit of lanthana in ceria lies within this range. That the lattice parameter did not exhibit a constant maximum value with increasing lanthana content is attributed to overlap of the displaced peaks characteristic of the solid solution in ceria with those of a hexagonal close-packed (*hcp*) structure characteristic of lanthana, also formed in the composition range $0.6 < x < 0.9$. Further resolution of the complex XRD patterns observed over the composition range of $0.6 < x < 0.9$ was beyond this study—the primary interest being the two solid solutions. The *hcp* structure of lanthana was the sole constituent of the XRD patterns in the range $0.9 < x < 1$. It is concluded that the limit of the second solid solution, that of ceria in lanthana, is about 10 cation % cerium ($x = 0.9$)—again in agreement with the literature

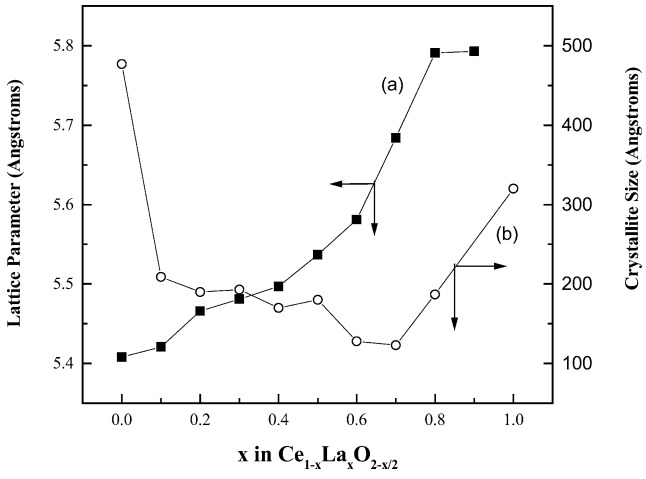


Fig. 1. Lattice parameter (a) and crystallite size (b) as functions of $x$, the atomic fraction of lanthanum in $Ce_{1-x}La_xO_{2-x/2}$.

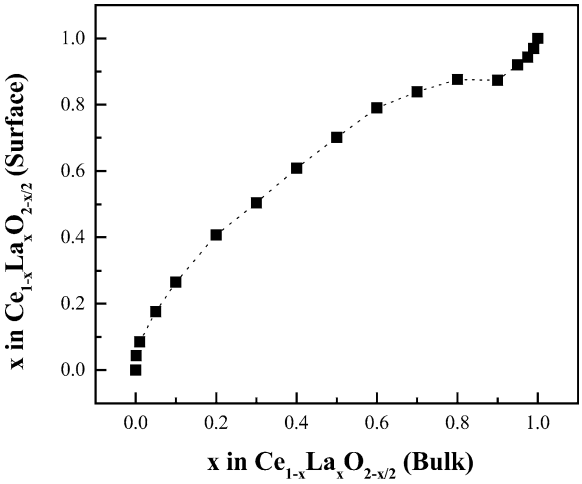


Fig. 2. The composition of the surface as a function of the composition of the bulk mixed oxide where $x$ is the lanthanum cation fraction as in $Ce_{1-x}La_xO_{2-x/2}$.

values [4]. A progressive shift of the *hcp* peaks toward higher $2\theta$ values as $x$ was decreased from 1 to 0.9 is attributed to contraction of the lattice caused by the incorporation of the smaller ions of the ceria solute into the lanthana lattice. Crystallite sizes were based on the 220 XRD reflection found in a range of $2\theta$ values below the 47.6° peak observed for pure ceria. To improve resolution, the scans to measure line broadening were made separately from those for phase analysis being recorded for 1 h over a range of 15° in $2\theta$ centred on the 220-peak position. Compared with pure ceria, the results, presented in Fig. 1b, show a marked decrease in crystallite size relative to ceria over the range $x = 0.1$–$0.6$, whereas above 0.6 there is a marked increase probably reflecting the change to the hcp structure. In summary, $x < 0.6$ results in lanthana dissolved on ceria, $0.6 < x < 0.9$ results in mixed phases, and $x > 0.9$ results in ceria dissolved in lanthana.

Table 5
The surface and bulk compositions of the mixed oxides in terms of atomic fractions

| Bulk La $x_b$ | Bulk Ce $1-x_b$ | Surface La $x_s$ | Surface Ce $1-x_s$ | Enrichment factor $x_s/x_b$ |
|---|---|---|---|---|
| 0.001 | 0.999 | 0.044 | 0.956 | 44.00 |
| 0.01 | 0.99 | 0.085 | 0.915 | 8.50 |
| 0.05 | 0.95 | 0.176 | 0.824 | 3.52 |
| 0.1 | 0.9 | 0.265 | 0.735 | 2.65 |
| 0.2 | 0.8 | 0.407 | 0.593 | 2.04 |
| 0.3 | 0.7 | 0.504 | 0.496 | 1.68 |
| 0.4 | 0.6 | 0.609 | 0.391 | 1.52 |
| 0.5 | 0.5 | 0.701 | 0.299 | 1.40 |
| 0.6 | 0.4 | 0.790 | 0.210 | 1.32 |
| 0.7 | 0.3 | 0.839 | 0.161 | 1.20 |
| 0.8 | 0.2 | 0.876 | 0.124 | 1.10 |
| 0.9 | 0.1 | 0.873 | 0.127 | 0.97 |
| 0.95 | 0.05 | 0.920 | 0.080 | 0.97 |
| 0.975 | 0.025 | 0.943 | 0.057 | 0.97 |
| 0.99 | 0.01 | 0.969 | 0.031 | 0.98 |

### *3.3.2. Surface compositions*

Aliquots of the same preparations of mixed oxides were analysed by XPS to determine the surface ionic fractions of cerium and lanthanum. The experimental results are presented in Fig. 2 and in Table 5, where the lanthanum surface enrichment factor (the ratio of surface lanthanum to bulk lanthanum) provides a convenient measure of preferential segregation to the surface. In outline, the surface of the lanthana-in-ceria solutions are enriched in lanthanum, the ceria-in-lanthana solutions are enriched in cerium, and where mixed phases are formed there is a tendency for lanthanum to segregate to the surface.

## 4. Discussion

Equilibrium surface segregation, as achieved in the methods used here, can be described as an adsorption phenomenon in which the solute atoms are bonded to the interface by some mechanism [14]. The simplest sort of adsorption theory is that due to Langmuir for a two-component system consisting of bulk and surface sites of one type only. The resulting adsorption isotherm would exhibit a constant enthalpy of segregation, independent of the surface coverage by the segregating solute.

We shall limit this discussion to classifying segregation from those ranges of the bulk composition which form solid solutions: that is, $0 < x < 0.6$, forming solid solution of Lithuania in a ceria matrix, and $0.9 < x < 1.0$, forming solid solutions of ceria in a lanthana matrix. When considering the isotherms, it is convenient to describe compositions in terms of the atomic fractions of the solute. To retain "$x$" to quantify the atomic fraction of lanthanum in the ceria matrix, the atomic fraction of ceria in lanthana as solvent will be designated as "$y$;" thus, the relevant ranges of compositions of the two solid solutions are $0 < x < 0.6$ and $0 < y < 0.1$, respectively. For the lanthana-in-ceria case, where several data

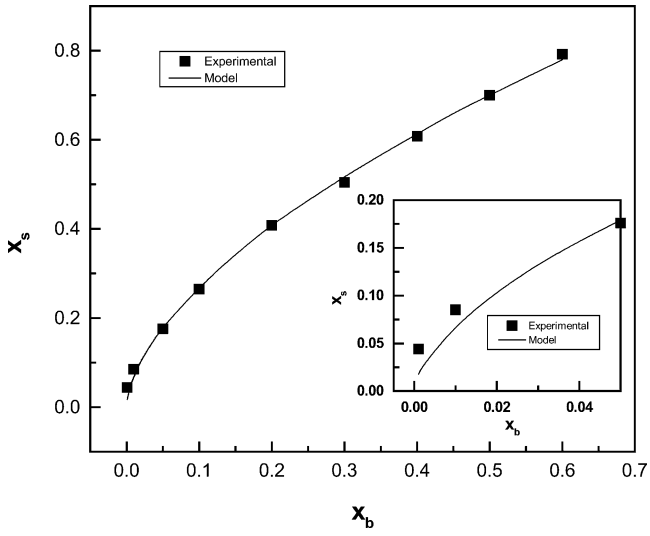


Fig. 3. A comparison of the measured and modelled compositions of the surface, $x_s$, as a function of the composition of the bulk mixed oxide, $x_b$, where $x_s$ and $x_b$ are the lanthanum cation fractions as in $Ce_{1-x}La_xO_{2-x/2}$.

points have been established, adoption of a power law to correlate the surface and bulk compositions achieves a very good fit. The isotherm takes the form

$$x_s = 1.06x_b^{0.6},$$

where $x_s$ and $x_b$ are the ionic fractions of lanthanum in the surface and bulk composition, respectively. Experimental (points) and model (line), achieving a percentage fit of 99.8, are compared in Fig. 3. For the ceria-in-lanthana case, where few experimental points are available, the equation is

$$y_s = 1.32y_b^{0.9},$$

where $y_s$ and $y_b$ are the ionic fractions of lanthanum in the surface and bulk composition, respectively. The percentage fit is 98.2, demonstrating only consistency with the power law rather than further proof of it.

Such power laws are similar in form to the Freundlich isotherm widely used to describe the effect of pressure on the adsorption of gases onto surfaces. Perusal of Fig. 3 (inset) shows the model to be in error in dilute solutions where $x_s < 0.05$: the model underestimates the extent of surface segregation. One plausible explanation for this is that surfaces are generally not atomically smooth; thus, a segregating species will react first and most energetically with sites exhibiting high coordinative unsaturation; for example, at low coverages there may be disproportionately high contributions from disordered segregation at steps, ledges, and other surface defects. Species segregating subsequently will not adsorb so strongly. The essential point is that the this form of the segregation isotherm suggests, in contrast to the tenets of the Langmuir isotherm, that free energies of segregation vary with surface composition.

## 5. Conclusion

The measured relationship between the equilibrium compositions of the surface and bulk of the solid solutions formed by the mixed oxides of ceria and lanthana lends itself to an empirical quantitative expression similar in form to the Freundlich adsorption isotherm.

## References

[1] Y. Osada, S. Koike, T. Fukushima, T. Ogasawara, T. Shikada, T. Ikariya, Appl. Catal. 59 (1990) 59.
[2] K. Otsuka, M. Kunitomi, J. Catal. 105 (1987) 525.
[3] W.C. Mackrodt, M. Fowles, M.A. Morris, US patent 4,940,685.
[4] V.R. Choudhary, V.H. Rane, J. Catal. 130 (1991) 411.
[5] G. Rienacker, Y. Wu, Z. Anorg. Allg. Chem. 315 (1962) 121.
[6] M.F. Wilkes, P. Hayden, A.K. Bhattacharya, Appl. Surf. Sci. (in press).
[7] M.F. Wilkes, P. Hayden, A.K. Bhattacharya, J. Catal. (Parts I and II, in press).
[8] J.M. Scofield, J. Electron. Spectrosc. Relat. Phenom. 8 (1976) 129.
[9] R.F. Reilman, A. Msegane, S.T. Manson, J. Electron. Spectrosc. Relat. Phenom. 8 (1976) 389.
[10] M.P. Seah, W.A. Dench, Surf. Int. Anal. 1 (1979) 2.
[11] M.P. Seah, Surf. Int. Anal. 2 (1980) 2222.
[12] T. Kudo, H. Obayashi, J. Electrochem. Soc.: Solid State Sci. Technol. 122 (1975) 142.
[13] D.-J. Kim, J. Am. Ceram. Soc. 72 (8) (1989) 1415;
S.J. Hong, A.V. Virkar, J. Am. Ceram. Soc. 78 (2) (1995) 433.
[14] P. Wynblatt, R.C. McCune, in: J. Nowotny, L.-C. Dufour (Eds.), Surface and Near Surface Chemistry of Oxide Materials, Elsevier, Amsterdam, 1988, p. 247.
[15] P.G. Harrison, D.A. Creaser, B.A. Wolfindale, K.C. Waugh, M.A. Morris, W.C. Mackrodt, in: T.J. Dines, C.H. Rochester, J. Thomson (Eds.), Catalysis and Surface Characterisation, 1992, ISBN 0-85186-335-3.
[16] H. Inaba, H. Tagawa, Solid State Ionics 83 (1996) 1.
[17] B.D. Cullity, Elements of X-ray Diffraction, Addison–Wesley, Reading, MA, 1959.